Unperturbed Expression Bias of Imprinted Genes in Schizophrenics

Attila Gulyás-Kovács[‡], Ifat Keydar[‡], ..., Andrew Chess[*]

Icahn School of Medicine at Mount Sinai

‡ equal contribution; ∗ correspondence: andrew.chess@mssm.edu

Contents

1   Main text

How inter-individual differences in gene regulation correlates with disease is beginning to be examined through analyses of RNA-seq from post-mortem brains of individuals with schizophrenia and from control brains [6]. Here we focus on differences in allele-specific expression, following up on the CommonMind Consortium (CMC http://www.synapse.org/CMC) RNA-seq analyses of > 500 human dorsolateral prefrontal cortex (DLPFC) samples. We find that the fraction of imprinted human genes is consistent with lower ($\approx 0.5\%$) [1, 2, 3, 5, 13] as opposed to higher [8] estimates in mice. The handful of novel potentially imprinted genes we find are all in close genomic proximity to known imprinted genes. Analyzing the extent of allelic expression bias—a hallmark of imprinting—across hundreds of individuals allowed us to examine its dependence on various factors. We find that allelic bias is independent of the diagnosis of schizophrenia. In contrast age up or down-regulates allelic bias of some imprinted genes and genetic ancestry also has an impact.

The observation [12, 14] that maternally derived microduplications at 15q11-q13—harboring the imprinted gene UBE3A—may not only cause Prader-Willi syndrome, but are also highly penetrant for schizophrenia has raised the possibility that perturbation of regulation of imprinted genes in general may play a role in psychotic disorders. As it is known that the extent of imprinting of individual genes varies over different tissues we chose the DLPFC region, which controls complex cognitive and executive functions and is known to display functional abnormalities in schizophrenia. We obtained pre-publication DLPFC RNA-seq data from the CMC and analyzed allele-specific expression with the idea of (i) identifying imprinted genes in the adult human brain and (ii) explaining the variability in allelic bias across 579 individuals in terms of their psychiatric diagnosis, age at death, etc. This was facilitated by the balanced case-control groups (258 SCZ, 267 Control, 54 bipolar or other affective/mood disorder, AFF) and the large age variability.

For each individual i and gene g we quantified allelic bias based on RNA-seq reads using a statistic called *read count ratio* S_{ig} (Fig. 1, Methods), which ranges from 0.5 to 1 indicating unbiased biallelic expression (at 0.5), some allelic bias (at intermediate values) or strictly monoallelic expression (at 1). We corrected for a number of factors this approach is known to be sensitive to. We quality-filtered RNA-seq reads and helped distinguish allele-specific reads using DNA genotyping data before calculating S and then applied post hoc corrections for mapping bias (Methods).

Of 15584 genes with RNA-seq data 5307 genes passed our filters designed to remove genes with scarce RNA-seq data reflecting low expression and/or low coverage of RNA-seq (Methods, Section 2.5). Fig. 2 presents the conditional empirical distribution of $S_{\cdot g}$ across all individuals given each gene g. The observed wide $S_{\cdot g}$ distributions suggest large across-individuals variation of allelic bias for all genes, even if a substantial component of the $S_{\cdot g}$ variation originates from technical sources. Still, as expected, for many genes known to be imprinted in mice or in other human tissues (referred to as *known imprinted* genes like PEG10, ZNF331) the distribution of $S_{\cdot g}$ was shifted to the right signaling strong allelic bias (Fig. 2, upper half).

To identify imprinted genes in the human adult DLPFC we defined the score of each gene g as the fraction of individuals i for whom $S_{ig} > 0.9$. We ranked all 5307 genes according to their score (Fig. 2 bottom right). The heat map of the $S_{\cdot g}$ distribution for ranked genes (Fig. 2, lower left) shows that the top 50 genes, which constitute $\approx 1\%$ of all genes in our analysis, are qualitatively different from the bottom $\approx 99\%$ exhibiting strongly right-shifted distribution of $S_{\cdot g}$ characteristic to imprinting.

29 of the top-scoring 50 genes fell into previously described imprinted gene clusters (Fig. S1); 21 of these 29 are *known imprinted* genes while 8 are *nearby candidates* defined as genes near *known*

imprinted ones but themselves previously not shown to be imprinted (blue and green *y*-axis labels in Fig. 3). *A priori* the expectation is that *known imprinted* genes and *nearby candidates* are much more likely to be imprinted in the present data set than *distant candidates* defined as genes that neither belong to nor localize near ($<$ 1Mb) *known imprinted* genes (Fig. 3, red *y*-axis labels). We combined this prior expectation with two tests based on our data to distinguish imprinting from alternative causes of high read count ratio such as mapping bias and cis-eQTL effects [2] (see Methods: Reference/non-reference allele test and Test for nearly unbiased allelic expression). The results of both tests (X's and black bars, Fig. 3) agreed well with the *a priori* expected status. This prompted us to call imprinted in the adult human DLPFC all *known imprinted* and *nearby candidate* genes within the top 50. We included also the *known imprinted* gene UBE3A, which ranked below 50 but whose score was still substantial (Fig. S2) yielding 30 imprinted genes (panel headers in Fig. 4-5).

Getting at the central question of our work Fig. 4 shows that read count ratio is similarly distributed in the Control, SCZ and AFF group for all 30 imprinted genes suggesting independence between allelic bias and diagnosis of schizophrenia.

To show this quantitatively we fitted several fixed and mixed effects models [9] that model the dependence of read count ratio jointly on all explanatory variables (Methods, Section 2.9-2.12). Such joint models can capture much of the complex pattern of dependencies in genomic data including those we observed within and between technical and biological explanatory variables (Table S1, Fig. S3). For both the fixed and mixed class we selected the model that fitted the data the best (unlm.Q/wnlm.Q for both fixed and mixed models, Fig. S6, S7, S8). Fixed and mixed models also agreed qualitatively on gene-specific coefficients reporting effects/dependencies (Fig S10, S9). We based final inference on the selected mixed model because that gains power from letting genes "borrow strength from each other" (Fig. S5).

Based on the best fitting mixed model (henceforth "the model") we could formally reject the hypotheses that read count ratio depends on diagnosis as either main effect or interaction (see term (1 | Dx) and (1 | Dx : Gene) in Table 1, respectively). That this key result is not due to low power is indicated by the highly significant dependence of read count ratio on gene identity (see (1 | Gene) in Table 1 and compare panels in Fig. 4).

Fig. 5 and S4 suggest that the read count ratio depends negatively on age for some imprinted genes, depends positively for others, and is independent of age for the rest of imprinted genes. This apparent dependence might be indirect, i.e. one that is mediated by some variable(s) "inbetween" age and read count ratio (Fig. S3, S5) but the model allowed us to isolate the direct component of age dependence: we found that the gene-specific random age effect is indeed significant even if no fixed effect—which would be shared by all imprinted genes—was supported (see (Age | Gene) and Age, respectively, in Table 1).

Based on the model we also predicted gene-specific regression coefficients mediating the direct component of age effect (Fig. S10 top middle). The predicted coefficients agreed well with all but a few panels of Fig. 5 the latter of which (e.g. UBE3A) therefore represent purely indirect dependence.

The same type of analysis on the effects of ancestry principal components and gender gave similar results: while the fixed effect, shared by all genes, of these variables was negligible, three of the random, gene-specific, effects received significant support. These three, ordered by decreasing statistical significance, are (Ancestry.1 | Gene), (Ancestry.3 | Gene) and (1 | Gender : Gene) (Table 1). The corresponding predicted random coefficients are presented in Fig. S10.

In summary age, ancestry, and to a lesser extent gender, are suggested by our model-based analysis to exert effect on allelic bias in a way that the direction and magnitude of the effect varies

4

across genes.

The number of imprinted genes in the mammalian brain has been controversial: some early genome wide studies [8, 7] estimated over a thousand, suggesting that the number of imprinted genes in the brain is an order of magnitude greater than in other tissues. Later work cast doubt on the methodology used and found that the number of imprinted genes in brain is in line with expectations from studies of other tissues, identifying only a handful of new candidate imprinted genes in brain [3, 5, 13]. Based on 579 postmortem human DLPFC samples we find evidence supporting only a handful of novel imprinted genes all of which reside in genomic locations nearby to known imprinted genes. Thus our results support those more recent studies that found no large excess of imprinted genes in the brain.

The large size of our sample and the case-control makeup allowed us to explore the potential for correlation of extent of imprinting in the DLPFC with schizophrenia. Although our approach gave strong support for dependence of imprinting on age and ancestry, no dependence on schizophrenia was detected either when we assumed that the dependence is the same for all imprinted genes or that it varies across genes. Thus our data indicate that imprinting in the DLFPC does not play a significant role in schizophrenia in contradiction of the "imprinted brain" hypothesis [4]. Given the complex genetic architecture of schizophrenia [15] as well as technical noise in postmortem brain RNA studies there could still be some correlation of the extent of imprinting and schizophrenia.

We found that imprinting depends on ancestry in a gene specific manner but the type of dependence that is shared by all imprinted genes was not supported. This is expected because the studied ancestry variables must incorporate some of the cis expression QTLs in imprinted genes such that those eQTLS perturb allelic bias in a gene specific manner.

Our finding that imprinting depends on age in later adulthood is rather intriguing given the quantitative relationship between epigenetics and aging [10]. Age dependence of imprinting through early postnatal life supported experimentally [13] but such dependence during later adulthood has so far only been predicted [16] based on a hypothesis that links "genomic imprinting and the social brain" [11]. Previous genomics studies [3] were statistically underpowered to address this question in humans. Although our age-related finding supports the "social brain" hypothesis, it leaves the possibility open that the observed age related changes indicate merely the loss of tight regulation of those genes with aging.

2 Methods

2.1 Defining the read count ratio to quantify allelic bias

We quantified allelic bias based on RNA-seq reads using a statistic called *read count ratio S*, whose definition we based on the total read count T and the *higher read count* H, i.e. the count of reads carrying only either the reference or the alternative SNP variant, whichever is higher. The definition is

$$S_{ig} = \frac{H_{ig}}{T_{ig}} = \frac{\sum_s H_s}{\sum_s T_s}, \tag{1}$$

where i identifies an individual, g a gene, and the summation runs over all SNPs s for which gene g is heterozygous in individual i (Fig. 1). Note that if B_{ig} is the count or reads that map to the b_{ig} allele (defined as above) and if we make the same distributional assumption as above, namely that $B_{ig} \sim \mathrm{Binom}(p_{ig}, T_{ig})$, then $\Pr(H_{ig} = B_{ig}|p_{ig})$, the probability of correctly assigning the reads with the higher count to the allele towards which expression is biased, tends to 1 as $p_{ig} \to 1$. We took advantage of this theoretical result in that we subjected only those genes to statistical inference, whose read count ratio was found to be high and, therefore, whose p_{ig} is expected to be high as well.

Fig. 1 illustrates the calculation of S_{ig} for the combination of two hypothetical genes, g_1, g_2, and two individuals, i_1, i_2. It also shows an example for the less likely event that the lower rather than the higher read count corresponds to the SNP variant tagging the higher expressed allele (see SNP s_3 in gene g_1 in individual i_2).

Before we carried out our read count ratio-based analyses, however, we cleaned our RNA-seq data by quality-filtering and by improving the accuracy of SNP calling with the use of DNA SNP array data and imputation. In the following subsections of Methods we describe the data, these procedures, as well as our regression models in detail.

2.2 Brain samples, RNA-seq

Human RNA samples were collected from the dorsolateral prefrontal cortex of the CommonMind consortium from a total of 579 individuals after quality control. Subjects included 267 control individuals, as well as 258 with schizophrenia (SCZ) and 54 with affective spectrum disorder (AFF). RNA-seq library preparation uses Ribo-Zero (which selects against ribosomal RNA) to prepare the RNA, followed by Illumina paired end library generation. RNA-seq was performed on Illumina HiSeq 2000.

2.3 Mapping, SNP calling and filtering

We mapped 100bp, paired-end RNA-seq reads ($\approx$ 50 million reads per sample) using Tophat to Ensembl gene transcripts of the human genome (hg19; February, 2009) with default parameters and 6 mismatches allowed per pair (200 bp total). We required both reads in a pair to be successfully mapped and we removed reads that mapped to > 1 genomic locus. Then, we removed PCR replicates using the Samtools rmdup utility; around one third of the reads mapped (which is expected, given the parameters we used and the known high repeat content of the human genome). We used Cufflinks to determine gene expression of Ensembl genes, using default parameters. Using the BCFtools utility of Samtools, we called SNPs (SNVs only, no indels). Then, we invoked a

quality filter requiring a Phred score > 20 (corresponding to a probability for an incorrect SNP call < 0.01).

We annotated known SNPs using dbSNP (dbSNP 138, October 2013). Considering all 579 samples, we find 936,193 SNPs in total, 563,427 (60%) of which are novel. Further filtering of this SNP list removed the novel SNPs and removed SNPs that either did not match the alleles reported in dbSNP or had more than 2 alleles in dbSNP. We also removed SNPs without at least 10 mapped reads in at least one sample. Read depth was measured using the Samtools Pileup utility. After these filters were applied, 364,509 SNPs remained in 22,254 genes. These filters enabled use of data with low coverage. For the 579 samples there were 203 million reads overlapping one of the 364,509 SNPs defined above. Of those 158 million (78%) had genotype data available from either SNP array or imputation.

2.4   Genotyping and calibration of imputed SNPs

DNA samples were genotyped using the Illumina Infinium SNP array. We used PLINK with default parameters to impute genotypes for SNPs not present on the Infinium SNP array using 1000 genomes data. We calibrated the imputation parameters to find a reasonable balance between the number of genes assessable for allelic bias and the number false positive calls since the latter can arise if a SNP is incorrectly called heterozygous.

We first examined how many SNPs were heterozygous in DNA calls and had a discordant RNA call (i.e. homozygous SNP call from RNA-seq) using different imputation parameters. Known imprinted genes were excluded. We examined RNA-seq reads overlapping array-called heterozygous SNPs which we assigned a heterozygosity score L_{het} of 1, separately from RNA seq data overlapping imputed heterozygous SNPs, where the L_{het} score could range from 0 to 1. After testing different thresholds we selected an L_{het} cutoff of 0.95 (i.e. imputation confidence level of 95%), and a minimal coverage of 7 reads per SNP. With these parameters, the discordance rate (monoallelic RNA genotype in the context of a heterozygous DNA genotype) was 0.71% for array-called SNPs and 3.2% for imputed SNPs.

The higher rate of discordance for the imputed SNPs is due to imputation error. These were taken into account in two ways. First, we considered all imputed SNPs for a gene g and individual i jointly. Second, we excluded any individual, for which one or more SNPs supported biallelic expression.

2.5   Quality filtering

Two kind of data filters were applied sequentially: (1) a *read count-based* and (2) an *individual-based*. The read count-based filter removes any such pair (i, g) of individual i and genes g for which the total read count $T_{ig} < t_{\mathrm{rc}}$, where the read count threshold t_{rc} was set to 15. The individual-based filter removes any genes g (across all individuals) if read count data involving g are available for less than t_{ind} number of individuals, set to 25. These final filtering procedures decreased the number of genes in the data from 15584 to $n = 5307$.

2.6 Reference/non-reference allele test to correct for mapping bias and eQTLs

We designed this test to distinguish imprinting from alternative causes of high read count ratio (Fig. 3): mapping bias or cis-eQTL effects. For any given gene this is a possibly compound test since there may be multiple SNPs that are informative for the read count ratio (see Defining the read count ratio above).

For a given gene the compound null hypothesis is that the observed high read count ratio is due only to imprinting. For each informative SNP this hypothesis means that the reference and non-reference allele are associated with equal probability to the *higher read count* [2] (see Methods: Defining the read count ratio to quantify allelic bias). Thus for each SNP we assumed that the number of individuals for whom the reference allele is associated to the *higher read count* is binomially distributed with probability parameter 0.5. The we calculated the fraction of informative SNPs for which the null hypothesis can be rejected at 0.05 significance level and used this information to decide whether the compound null hypothesis for the gene itself can be rejected.

2.7 Test for nearly unbiased allelic expression

The null hypothesis of this test is that the higher read count $H_{ig} = S_{ig}T_{ig}$ for gene g and individual i is drawn from a binomial distribution with a probability parameter $p_{ig} \approx 0.5$ suggesting nearly unbiased allelic expression. More specifically, the test was defined by the criteria

$$S_{ig} \leq 0.6 \text{ and } \text{UCL}_{ig} \leq 0.7, \tag{2}$$

where the 95% upper confidence limit UCL_{ig} for the expected read count ratio p_{ig} was calculated assuming that the higher read count $H_{ig} \sim \text{Binom}(p_{ig}, T_{ig})$, on the fact that binomial random variables are asymptotically (as $T_{ig} \to \infty$) normal with $\text{var}(H_{ig}) = T_{ig}p_{ig}(1 - p_{ig})$, and on the equalities $\text{var}(S_{ig}) = \text{var}(H_{ig}/T_{ig}) = \text{var}(H_{ig})/T_{ig}^2$. Therefore

$$\text{UCL}_{ig} = S_{ig} + z_{0.975}\sqrt{\frac{S_{ig}(1 - S_{ig})}{T_{ig}}}, \tag{3}$$

where z_p is the p quantile of the standard normal distribution.

2.8 Data transformations

We found transformations of the read count ratio data to be useful for fitting our statistical models (Section 2.9-2.12 below). We used either (or none) of the following two transformations:

1. The quasi-log transformation, defined as

$$\tau_Q(S_{ig}; T_{ig}) \equiv Q_{ig} = -\log\left(1 - S_{ig}\frac{T_{ig}}{T_{ig} + c}\right), \tag{4}$$

   where S_{ig} and T_{ig} mean read count ratio and total read count for individual i and gene g; log means natural logarithm (base e); c is a pseudo read count set to 1 in order to avoid zero in the parenthesis since the log function is undefined at 0.

2. The rank transformation

$$\tau_R(S_{ig}; \{S_{jg}\}_j) \equiv R_{ig} = \frac{\#\{j : S_{jg} \leq S_{ig}\}}{\#j} \times 100. \tag{5}$$

Note that j may equal i in Eq. 5. Thus, this transformation first ranks individual i among all individuals j and then scales the ranks between 0 and 100.

2.9 Statistical models: informal overview

We modeled the dependence of read count ratio of imprinted genes jointly on all biological and technical explanatory variables (Table S1) using several multiple regression models. Based on their structure our models can be classified into two sets of fixed and a set of mixed regression models (Fig. S5). Furthermore our models can be also classified based on non-structural properties (link function, error distribution, weighting, and the data transformation to read count ratio; see model classes in Table S2).

Fig. S5 explains that among the two fixed and the mixed structural model class the mixed one is both more powerful and robust because its random effects terms allow gene-specific parts of the model to "borrow strength from each other". The cost of the enhanced power in mixed models is the lack of estimates and confidence intervals (as well as p-values) for gene-specific coefficients (parameters), which the less powerful fixed models do provide (Fig. S9). Instead of being estimated, gene-specific coefficients in mixed models therefore can only be *predicted* without information on confidence surrounding them (see Fig. S10 for predicted gene-specific coefficients under a mixed model). Nonetheless, the low power and low robustness of fixed models became apparent from results like those in Fig. S9 so we based our final inference (Table 1) on mixed modeling. Note, however, that we found an overall qualitative agreement between mixed and fixed models regarding gene-specific coefficients (compare Fig S10 and S9).

To select the best model within the mixed structural class we compared model fit of the non-structural types (Fig. S8) and found that the unlm.Q and wnlm.Q types fitted the data the best. Similar results were obtained for fixed models (Fig. S6, S7).

2.10 Statistical models: formal overview

Our fixed and mixed effects multiple regression models are all generalized linear models (GLMs). GLMs in general describe a conditional distribution of a response variable y given a linear predictor η such that the distribution is from the exponential family and that $E(y|\eta) = g^{-1}(\eta)$, where g is some link function. In the present context the response y is the observed read count ratio that is possibly transformed to improve the model's fit to the data. We performed fitting with the lme4 and stats R packages and tested several combinations of transformations, link functions, and error distributions (Table S2). For inference we used the best fitting combination (unlm.Q, Table S2) as assessed by the normality and homoscedasticity of residuals (Fig. S8, also Fig. S6, S7) as well as by monitoring convergence.

In mixed GLMs the linear predictor $\eta = X\beta + Zb$ and in fixed GLMS $\eta = X\beta$, where X, Z are design matrices containing data on explanatory variables whereas β and b are fixed and random vectors of regression coefficients that mediate fixed and random effects, respectively (see Section 2.11 and Fig. S5 for details).

Besides the random effects term Zb the key difference between the mixed and fixed models in this study is that the former describes read count ratio *jointly* for all imprinted genes and the latter

9

separately for each imprinted gene. An important consequence is that our mixed models are more powerful because they can utilize information shared by all genes. Therefore we preferred mixed models for final inference and used fixed models only to guide selection among possible mixed models (Section 2.12).

2.11 Detailed syntax and semantics of mixed models

Here we describe the detailed syntax and semantics of the normal linear mixed models combined with a quasi-log transformation Q of read count ratio as this combination was found to provide the best fit (Fig. S8). We have data on 579 individuals and 30 imprinted genes and so the response vector is $y = (Q_{i_1 g_1}, ..., Q_{i_{579} g_1}, Q_{i_1 g_2}, ..., Q_{i_{579} g_2}, ..., Q_{i_1 g_{30}}, ..., Q_{i_{579} g_{30}})$. The model in matrix notation is

$$y \quad = \quad X\beta + Zb + \varepsilon \tag{6}$$

$$\varepsilon_i \quad \overset{\text{i.i.d.}}{\sim} \quad \mathcal{N}(0, \sigma^2), \ i = 1, ..., mn \tag{7}$$

$$b \quad \sim \quad \mathcal{N}(0, \Omega_b), \tag{8}$$

where the size of the covariance matrix Ω_b depends on the number of terms with random effects (the columns of Z). Simply put: errors and random coefficients are all normally distributed.

To clarify the semantics of Eq. 6 let us consider a simple toy model with just a few terms in the linear predictor. But before expressing it in terms of Eq. 6 it is easier to cast it in the compact "R formalism" of the stats and lme4 packages of the R language as

$$y \sim \overbrace{1 + \text{Age}}^{\text{fixed effect}} + \underbrace{\overbrace{(1 + \text{Age} + \text{Ancestry.1} \,|\, \text{Gene})}^{\text{random effects}}}_{k=1} + \underbrace{(1 \,|\, \text{Dx} : \text{Gene})}_{k=2}. \tag{9}$$

First note that the random effect term labeled with $k = 1$ can be expanded into $(1 \,|\, \text{Gene}) + (\text{Age} \,|\, \text{Gene}) + (\text{Ancestry.1} \,|\, \text{Gene})$. The '1's mean intercept terms: one as a fixed effect and two as random effects. The first random intercept term $(1 \,|\, \text{Gene})$ expresses the gene-to-gene variability in read count ratio (compare panels in Fig. 4 and 5), in other words the random effect of the Gene variable. The second random intercept term $(1 \,|\, \text{Dx} : \text{Gene})$ corresponds to the interaction between psychiatric diagnosis Dx and Gene; it can be interpreted as the Gene specific effect of Dx or—equivalently—as Dx specific gene-to-gene variability. This term is not likely to be informative as Fig. 4 suggests little Gene specific effect of Dx.

We see that Age appears twice: first as a fixed slope effect on y and second as a Gene specific random slope effect, denoted as $(\text{Age} \,|\, \text{Gene})$. The random effect appears to be supported by Fig. 5 because the dependence of read count ratio on Age varies substantially among genes but the fixed effect is not supported because the negative dependence seen for several genes is balanced out by the positive dependence seen for others. The model includes another random slope effect: $(\text{Ancestry.1} \,|\, \text{Gene})$ with a similar interpretation as $(\text{Age} \,|\, \text{Gene})$ but lacks a fixed effect of Ancestry.1.

Now we are ready to write the toy model as an expanded special case of Eq. 6 as

$$y_i = \overbrace{\beta_0 + \text{Age}_i \beta_1}^{\text{fixed effects}} + \underbrace{\overbrace{b_0^{(1)} + \text{Age}_i b_1^{(1)} + \text{Ancestry.1}_i b_2^{(1)}}^{\text{random effects}}}_{\text{Gene}_i} + \underbrace{b_0^{(2)}}_{\text{Dx}_i : \text{Gene}_i} + \varepsilon_i. \tag{10}$$

As in the earlier R formalism the terms of the linear predictor are grouped into fixed and random effects. Within the latter group we have two batches of terms indicated by the k super-scripts on the random regression coefficients $b_j^{(k)}$. The first batch $\{b_0^{(1)}, b_1^{(1)}, b_2^{(1)}\}$ corresponds to $\{(1 \,|\, \mathrm{Gene}), (\mathrm{Age} \,|\, \mathrm{Gene}), (\mathrm{Ancestry.1} \,|\, \mathrm{Gene})\}$ in Eq. 9, the second batch contains only $b_0^{(2)}$ corresponding to $(1 \,|\, \mathrm{Dx} : \mathrm{Gene})$.

Within the kth batch Eq. 10 contains only a single intercept coefficient $b_0^{(k)}$ and, if random slope terms are also present in the batch, only a single slope coefficient associated with the variable Age or Ancestry.1. This is because only a single level of the factor Gene or the composite factor Dx : Gene needs to be considered for the ith observation; these levels are denoted as Gene_i and $\mathrm{Dx}_i : \mathrm{Gene}_i$, respectively. Implicitly however, Eq. 10 contains the respective coefficients for all levels of these factors. For example, there are $n = 30$ intercept coefficients $b_j^{(1)}$ each of which corresponds to a given gene. So to generalize Eq. 10 we need J_k coefficients in the kth batch, where J_k is the product of the number of factor levels and one plus the number of random slope variables. This way we can provide the expansion of the general formula Eq. 6 using the semantics of the toy model (Eq. 9, 10) as

$$y_i = \overbrace{\sum_{j=0}^{J} x_{ij} \beta_j}^{\text{fixed effects}} + \overbrace{\sum_{k=1}^{K} \sum_{j=0}^{J_k} z_{ij}^{(k)} b_j^{(k)}}^{\text{random effects}} + \varepsilon_i. \tag{11}$$

2.12   Model fitting and selection

Eq. 11 describes a large set of mixed models that differ in one or more individual terms that constitute their linear predictor. From this set we aimed to select the best fitting model under the Akaike Information Criterion (AIC).

We used a heuristic search strategy in order to restrict the vast model space to a relatively small subset of plausible models. The search was started at a model whose relatively simple linear predictor was composed of terms using our prior results based on fixed effects models. The same results suggested a sequence in which further terms were progressively added to the model to test if they improve fit. Improvement was assessed by ΔAIC and the χ^2-test on the degrees of freedom that correspond the evaluated term. If fit improved the term was added otherwise it was omitted. Next, further terms were tested. This iterative procedure lead to the following model.

$$\begin{aligned}
Q \quad \sim \quad & \mathrm{RIN} + (1 \,|\, \mathrm{RNA\_batch}) + (1 \,|\, \mathrm{Institution}) + (1 \,|\, \mathrm{Institution} : \mathrm{Individual}) \\
+ \quad & (1 \,|\, \mathrm{Gene} : \mathrm{Institution}) + (1 \,|\, \mathrm{Gender} : \mathrm{Gene}) \\
+ \quad & (\mathrm{Age} + \mathrm{RIN} + \mathrm{Ancestry.1} + \mathrm{Ancestry.3} \,|\, \mathrm{Gene})
\end{aligned}$$

We refer to this as the "best fitting model" even thought it may represent only a local optimum in model space.

3   References

[1] Daniel Andergassen, Christoph P Dotter, Daniel Wenzel, Verena Sigl, Philipp C Bammer, Markus Muckenhuber, Daniela Mayer, Tomasz M Kulinski, Hans-Christian Theussl, Josef M Penninger, Christoph Bock, Denise P Barlow, Florian M Pauler, and Quanah J Hudson. Mapping the mouse allelome reveals tissue-specific regulation of allelic expression. *eLife*, 6, August 2017.

[2] Tomas Babak, Brian DeVeale, Emily K Tsang, Yiqi Zhou, Xin Li, Kevin S Smith, Kim R Kukurba, Rui Zhang, Jin Billy Li, Derek van der Kooy, Stephen B Montgomery, and Hunter B Fraser. Genetic conflict reflected in tissue-specific maps of genomic imprinting in human and mouse. *Nature genetics*, 47:544–549, May 2015.

[3] Yael Baran, Meena Subramaniam, Anne Biton, Taru Tukiainen, Emily K. Tsang, Manuel A. Rivas, Matti Pirinen, Maria Gutierrez-Arcelus, Kevin S. Smith, Kim R. Kukurba, Rui Zhang, Celeste Eng, Dara G. Torgerson, Cydney Urbanek, Jin Billy Li, Jose R. Rodriguez-Santana, Esteban G. Burchard, Max A. Seibold, Daniel G. MacArthur, Stephen B. Montgomery, Noah A. Zaitlen, and Tuuli Lappalainen. The landscape of genomic imprinting across diverse adult human tissues. *Genome Research*, 25(7), 2015.

[4] Bernard Crespi. Genomic imprinting in the development and evolution of psychotic spectrum conditions. *Biological reviews of the Cambridge Philosophical Society*, 83(4):441–93, nov 2008.

[5] Brian DeVeale, Derek van der Kooy, and Tomas Babak. Critical evaluation of imprinted gene expression by RNA-seq: A new perspective. *PLoS Genetics*, 8(3):e1002600, jan 2012.

[6] Menachem Fromer, Panos Roussos, Solveig K Sieberts, Jessica S Johnson, David H Kavanagh, Thanneer M Perumal, Douglas M Ruderfer, Edwin C Oh, Aaron Topol, Hardik R Shah, Lambertus L Klei, Robin Kramer, Dalila Pinto, Zeynep H Gümü, A Ercument Cicek, Kristen K Dang, Andrew Browne, Cong Lu, Lu Xie, Ben Readhead, Eli A Stahl, Jianqiu Xiao, Mahsa Parvizi, Tymor Hamamsy, John F Fullard, Ying-Chih Wang, Milind C Mahajan, Jonathan M J Derry, Joel T Dudley, Scott E Hemby, Benjamin A Logsdon, Konrad Talbot, Towfique Raj, David A Bennett, Philip L De Jager, Jun Zhu, Bin Zhang, Patrick F Sullivan, Andrew Chess, Shaun M Purcell, Leslie A Shinobu, Lara M Mangravite, Hiroyoshi Toyoshiba, Raquel E Gur, Chang-Gyu Hahn, David A Lewis, Vahram Haroutunian, Mette A Peters, Barbara K Lipska, Joseph D Buxbaum, Eric E Schadt, Keisuke Hirai, Kathryn Roeder, Kristen J Brennand, Nicholas Katsanis, Enrico Domenici, Bernie Devlin, and Pamela Sklar. Gene expression elucidates functional impact of polygenic risk for schizophrenia. *Nature neuroscience*, sep 2016.

[7] Christopher Gregg, Jiangwen Zhang, James E. Butler, David Haig, and Catherine Dulac. Sex-Specific Parent-of-Origin Allelic Expression in the Mouse Brain. *Science*, 329(5992):682–685, aug 2010.

[8] Christopher Gregg, Jiangwen Zhang, Brandon Weissbourd, Shujun Luo, Gary P Schroth, David Haig, and Catherine Dulac. High-resolution analysis of parent-of-origin allelic expression in the mouse brain. *Science (New York, N.Y.)*, 329(5992):643–8, aug 2010.

[9] Gabriel E Hoffman and Eric E Schadt. variancePartition: interpreting drivers of variation in complex gene expression studies. *BMC bioinformatics*, 17(1):483, nov 2016.

[10] Steve Horvath. DNA methylation age of human tissues and cell types. *Genome biology*, 14(10):R115, oct 2013.

[11] Anthony R Isles, William Davies, and Lawrence S Wilkinson. Genomic imprinting and the social brain. *Philosophical transactions of the Royal Society of London. Series B, Biological sciences*, 361(1476):2229–37, dec 2006.

[12] Abdul Noor, Lucie Dupuis, Kirti Mittal, Anath C. Lionel, Christian R. Marshall, Stephen W. Scherer, Tracy Stockley, John B. Vincent, Roberto Mendoza-Londono, and Dimitri J. Stavropoulos. 15q11.2 duplication encompassing only the UBE3a gene is associated with developmental delay and neuropsychiatric phenotypes. 36(7):689–693.

[13] Julio D Perez, Nimrod D Rubinstein, Daniel E Fernandez, Stephen W Santoro, Leigh A Needleman, Olivia Ho-Shing, John J Choi, Mariela Zirlinger, Shau-Kwaun Chen, Jun S Liu, and Catherine Dulac. Quantitative and functional interrogation of parent-of-origin allelic expression biases in the brain. *eLife*, 4:e07860, jan 2015.

[14] Elliott Rees, James T R Walters, Lyudmila Georgieva, Anthony R Isles, Kimberly D Chambert, Alexander L Richards, Gerwyn Mahoney-Davies, Sophie E Legge, Jennifer L Moran, Steven A McCarroll, Michael C O'Donovan, Michael J Owen, and George Kirov. Analysis of copy number variations at 15 schizophrenia-associated loci. *The British journal of psychiatry : the journal of mental science*, 204(2):108–14, feb 2014.

[15] Patrick F Sullivan, Mark J Daly, and Michael O'Donovan. Genetic architectures of psychiatric disorders: the emerging picture and its implications. *Nature Reviews Genetics*, 13(8):537–551, aug 2012.

[16] Francisco Ubeda and Andy Gardner. A model for genomic imprinting in the social brain: elders. *Evolution; international journal of organic evolution*, 66(5):1567–81, may 2012.

4   Acknowledgements

5 Author information

5.1 Affiliation

Attila Gulyás-Kovács[a]
Ifat Keydar[ab]
...
Andrew Chess[ac]

a Department of Genetics and Genomic Sciences, Department of Developmental and Regenerative Biology, Icahn School of Medicine at Mount Sinai, New York, NY 10029-6574

b current address: TODO

c Fishberg Department of Neuroscience, and Friedman Brain Institute, Icahn School of Medicine at Mount Sinai, New York, NY 10029-6574

5.2 Contributions

5.3 Competing financial interests

None

5.4 Corresponding author

Andrew Chess
email: andrew.chess@mssm.edu

6 Figures with legends
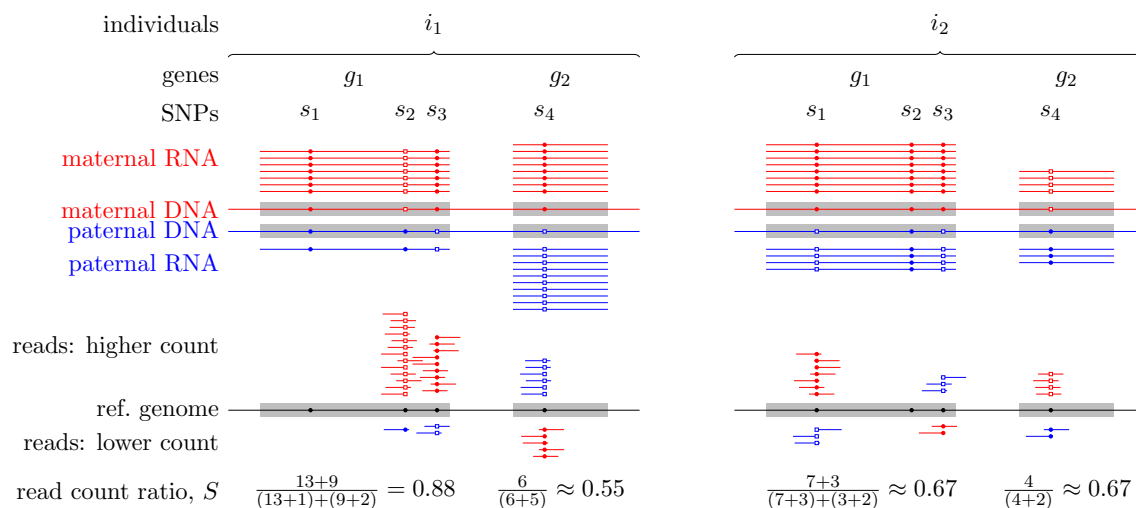
Figure 1: Quantifying allelic bias of expression in human individuals using the RNA-seq read count ratio statistic S_{ig}. The strength of bias towards the expression of the maternal (red) or paternal (blue) allele of a given gene g in individual i is gauged with the count of RNA-seq reads carrying the reference allele (small closed circles) and the count of reads carrying an alternative allele (open squares) at all SNPs for which the individual is heterozygous. The allele with the *higher read count* tends to match the allele with the higher expression but measurement errors may occasionally revert this tendency as seen for SNP s_3 in gene g_1 in individual i_2.
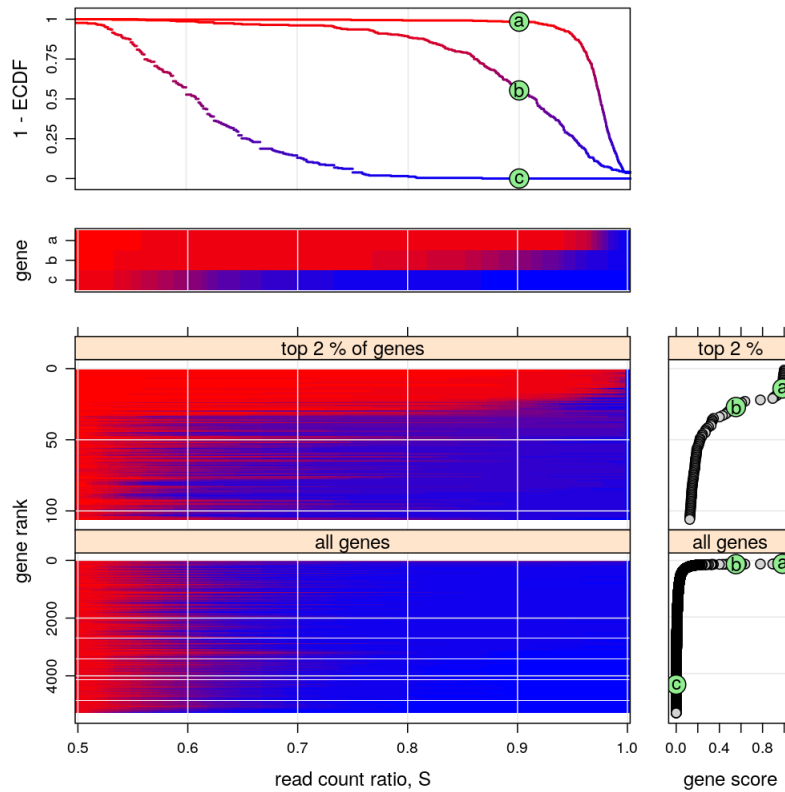
Figure 2: Across-individuals distribution of read count ratio S for each gene indicates substantial variation of allelic bias and that $< 1\%$ of all genes are imprinted. The vertically arranged four main panels present the empirical distribution of $S_{\cdot g}$ across all individuals given each gene g. The *upper two panels* are distinct representations (survival plot: $1 - \text{ECDF}$, and "survival heatmap") of the same three distributions corresponding to a: PEG10, b: ZNF331, and c: AFAP1. PEG10 and ZNF331, previously found to be imprinted in mice or in other human tissues, and one for AFAP1, a gene without prior evidence. The bottom two survival heatmaps present the distribution of $S_{\cdot g}$ for the top 2% and 100% of the 5307 analyzed genes. These are ranked according to gene score defined as $1 - \text{ECDF}(0.9)$ in the *bottom far right panels*. The score of PEG10, ZNF331, and AFAP1 is marked by a, b, c, respectively, in green circles. As expected, PEG10 and ZNF331 both score high and rank within the top 30 of all genes suggesting they are also imprinted in the present context, the adult human DLFPC. The bottom panels also indicate that $< 1\%$ of all genes might be imprinted.
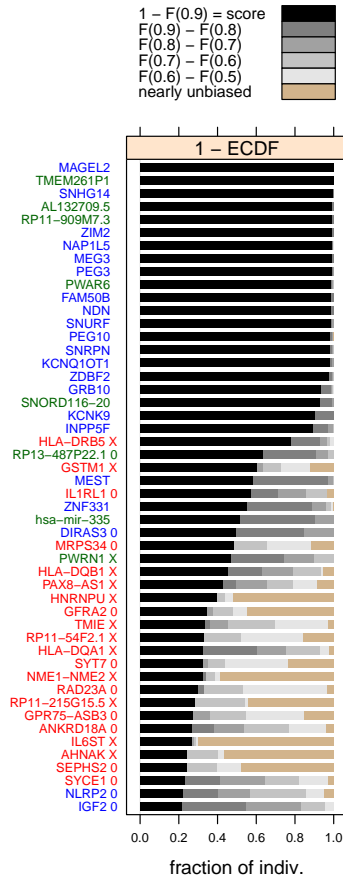
17

Figure 3: The top 50 genes ranked by the gene score defined, for gene g, as $1 - F_g(0.9)$, where F_g is the empirical cumulative distribution function (ECDF) for g. Thus $1 - F_g(0.9)$, is the fraction of individuals i for which $S_{ig} > 0.9$. Note that the same ranking and score is shown in the bottom half of Fig. 2. The tan colored bars indicate the fraction of individuals with nearly unbiased expression (Eq. 2). Gene names (y axis) are colored according to prior imprinting status: known imprinted (blue), nearby candidate (green), and distant candidate (red). "X" characters next to gene names indicate mapping bias and/or cis-eQTL effects based on the reference/non-reference allele test (Methods) while "0" indicates that total allele count was insufficient for this test.

18
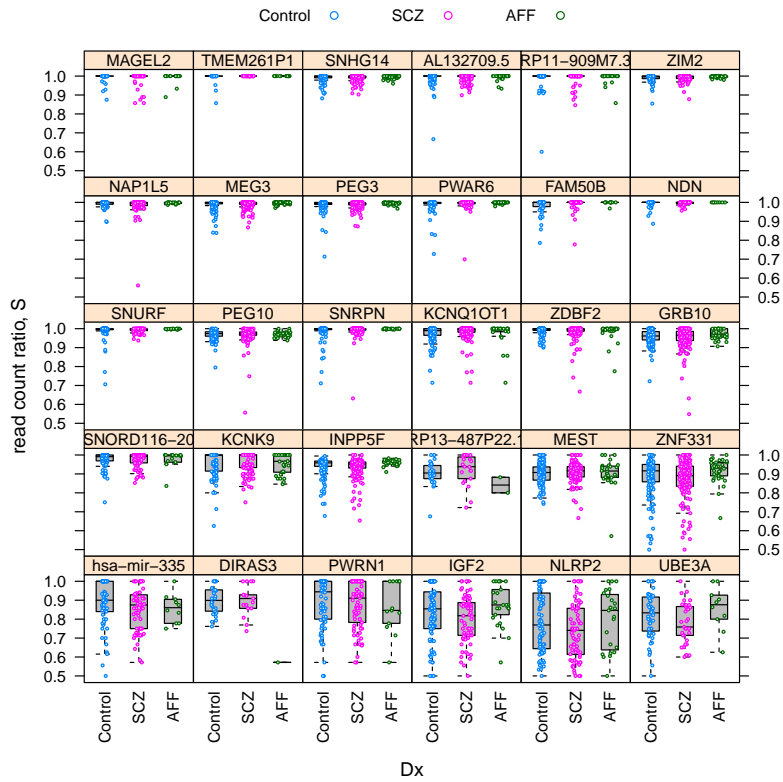
Figure 4: Schizophrenia does not affect allelic bias of imprinted genes. Distribution of read count ratio for Control, schizophrenic (SCZ), and affectic spectrum (AFF) individuals within each gene that has been considered as imprinted in the DLPFC brain area in this study.
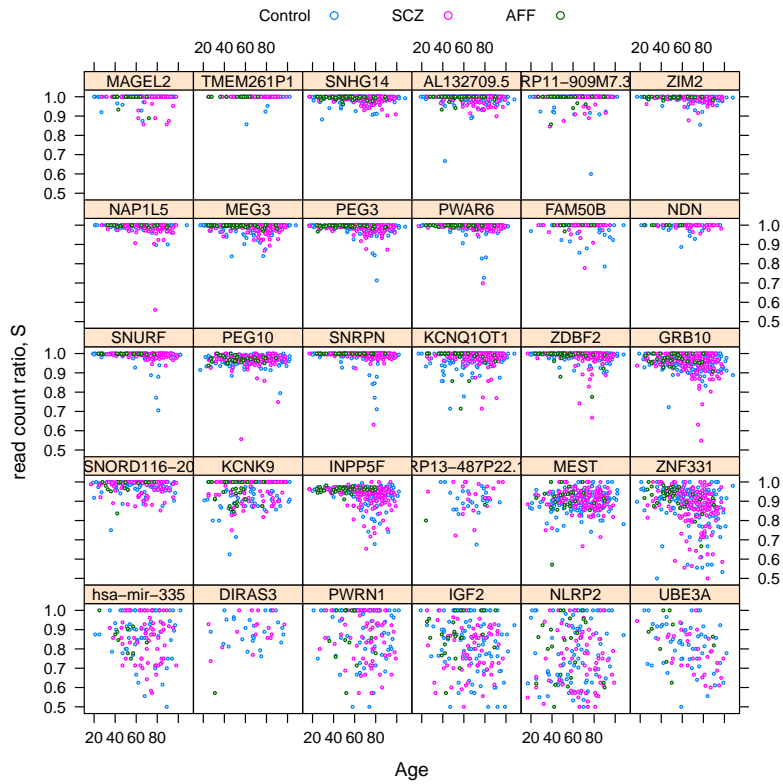
Figure 5: Allelic bias depends differentially on age across imprinted genes. The panels and colors are consistent with the imprinted genes and psychiatric diagnoses presented in Fig. 4. The differential dependence on age is apparent when comparing PEG3 or ZNF331 (negative dependence) to KCNK9 or RP13-487P22.1 (positive dependence) or to NDN or NLRP2 (no dependence).

20

7 Tables with legends

predictor term	interpretation	ΔAIC	p-value
$(1\,\vert\,\text{Gene})$	variability among genes	-126.8	8.5×10^{-28}
$(1\,\vert\,\text{Dx})$	variability among Control, SCZ, AFF	2.0	1.0
$(1\,\vert\,\text{Dx}:\text{Gene})$	Gene specific variability among Ctrl, SCZ, AFF	0.4	0.21
Age	effect of Age	1.3	0.39
$(\text{Age}\,\vert\,\text{Gene})$	Gene specific effect of Age	-18.9	2.5×10^{-5}
Ancestry.1	effect of Ancestry.1	0.6	0.24
$(\text{Ancestry.1}\,\vert\,\text{Gene})$	Gene specific effect of Ancestry.1	-71.2	4.6×10^{-16}
Ancestry.3	effect of Ancestry.3	1.6	0.54
$(\text{Ancestry.3}\,\vert\,\text{Gene})$	Gene specific effect of Ancestry.3	-17.9	3.8×10^{-5}
$(1\,\vert\,\text{Gender})$	difference between Male and Female	2.0	1.0
$(1\,\vert\,\text{Gender}:\text{Gene})$	Gene specific difference between M and F	-5.7	5.5×10^{-3}

Table 1: Dependence of read count ratio on various predictor terms in the mixed model; largely negative ΔAIC and small p-values indicate significant dependence (see Methods).

8 Supplementary information
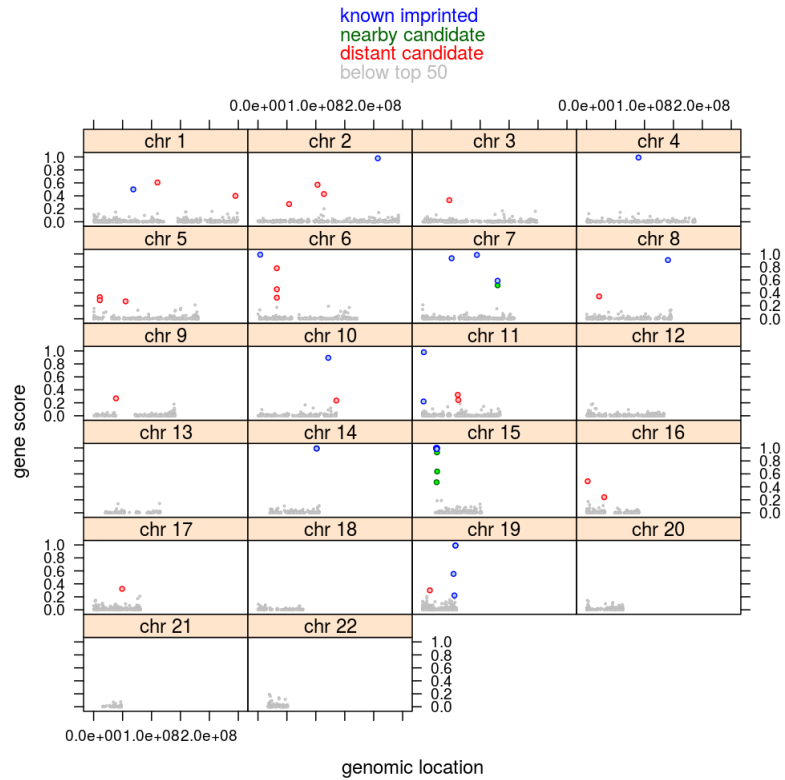
8.1 Supplementary figures with legends

Figure S1: Clustering of top-scoring genes in the context of human DLPFC around genomic locations that had been previously described as imprinted gene clusters in other contexts.
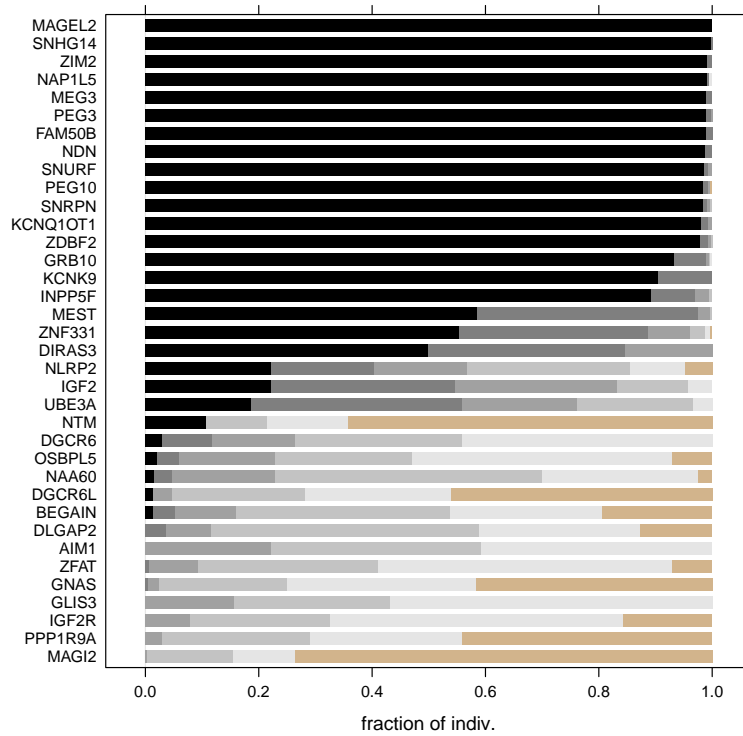
Known imprinted genes

Figure S2: Known imprinted genes ranked by the gene score (dark blue bars). "Known imprinted" refers to prior studies on imprinting in the context of any tissue and developmental stage. The length of the black bars indicates the fraction of individuals passing the test of nearly unbiased expression.
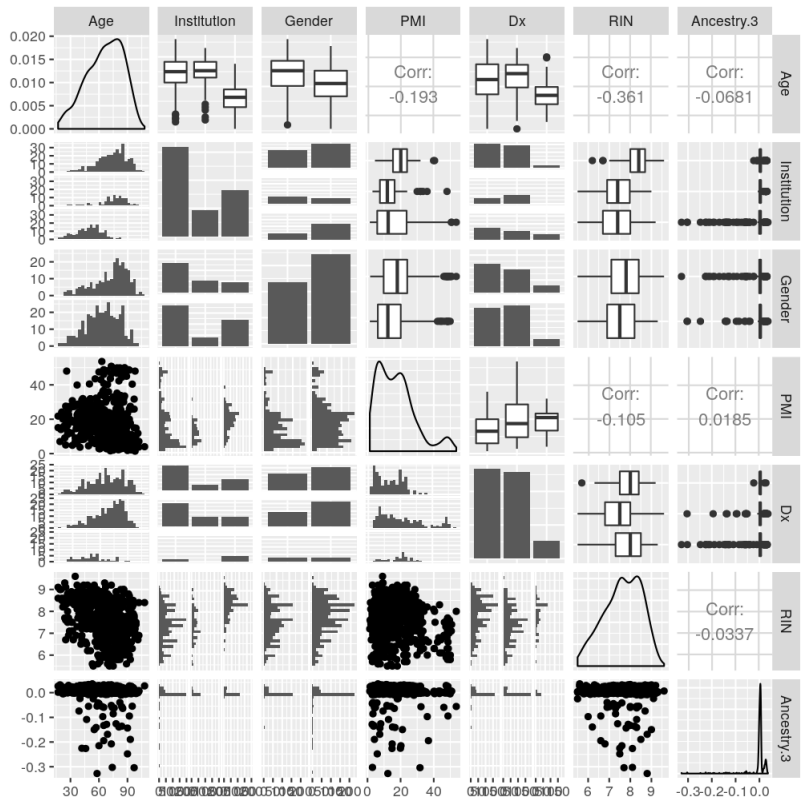
Figure S3: Distribution and inter-dependence of explanatory variables. The diagonal graphs of the plot-matrix show the marginal distribution of six variables (Age, Institution,...) while the off-diagonal graphs show pairwise joint distributions. For instance, the upper left graph shows that, in the whole cohort, individuals' Age ranges between ca. 15 and 105 years and most individuals around 75 years; the bottom and right neighbor of this graph both show (albeit in different representation) the joint distribution of Age and Institution, from which can be seen that individuals from Pittsburg tended to be younger than those from the two other institutions.
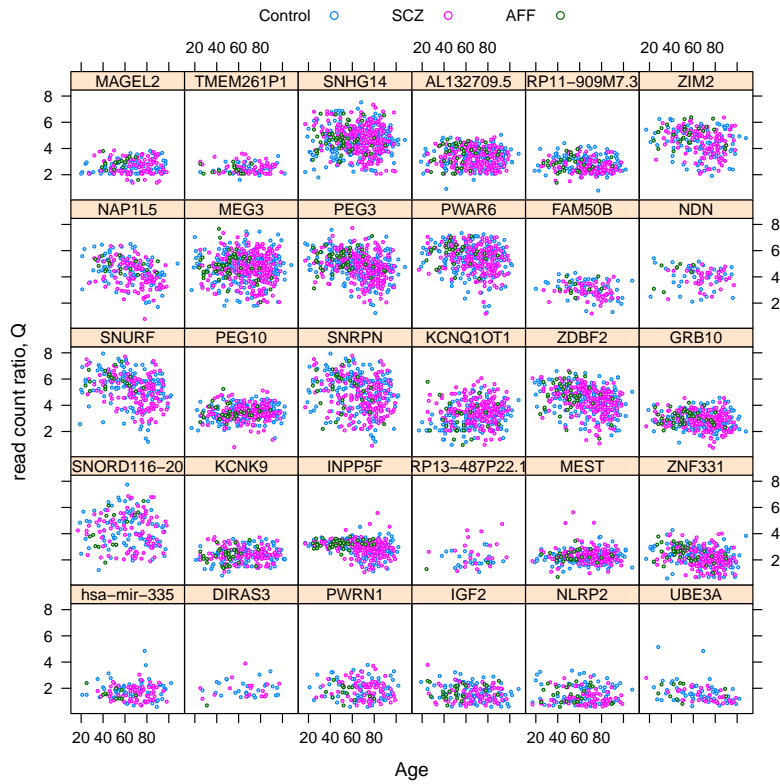
Figure S4: The quasi-log transformed read count ratio Q and age for imprinted genes. See Fig. 5 for the corresponding plots without quasi-log transformation and note that statistical inference was done based on the quasi log transformed data and not only age but several other explanatory variables (Table S1).
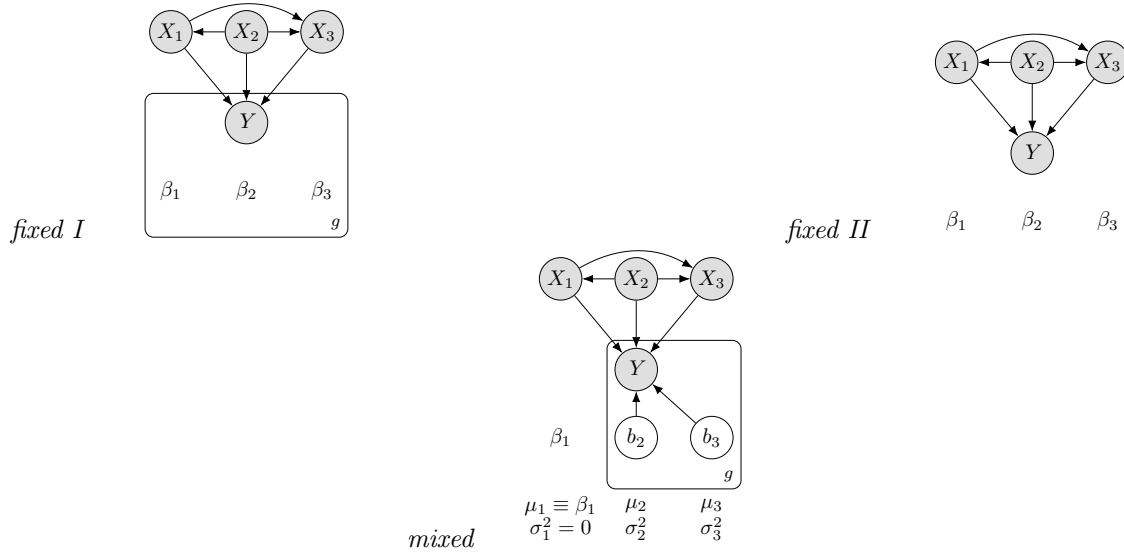
Figure S5: Three model structures: two *fixed* (upper left and right) and a *mixed* (lower middle) effects multiple regression model. In all three model structures the read count ratio Y_g—for several genes g—depends somehow on three explanatory variables X_j like Age or PMI (Table S1). For each gene g the probabilistic dependence is mediated by fixed $\beta_{1g}, \beta_{2g}, \beta_{3g}$ or random b_{2g}, b_{3g} regression coefficients. *fixed II* is a constrained version of the *fixed I* model structure such that $\beta_{jg_1} = \beta_{jg_2} = ... \equiv \beta_j$, which means that the effect of X_j on Y does not vary across genes in *fixed II*. The *mixed* model differs from *fixed I* in the way coefficients across genes vary for a given explanatory variable X_j. In the *fixed I* model structure there is no connection among $\beta_{jg_1}, \beta_{jg_2}, ...$, which means that the way Y_g, the read count ratio for gene g depends on variable X_j is completely separate from how the read count ratio for any other gene g' (i.e. $Y_{g'}$) depends on X_j. Consequently, the gene-specific substructures of *fixed I* contain no information on each other. This limitation is overcome with the *mixed* model structure because a set of coefficients across genes—e.g. the set $\{b_{2g}\}_g$—is modeled as a random sample from a normal distribution with parameters μ_2 and some $\sigma_2^2 > 0$. Thus μ_2 and σ_2^2 constitute information on the effect that is shared across all genes so that genes "borrow strength from each other". When $\sigma_j^2 = 0$ in the *mixed* model then all parameters $\{b_{jg}\}_g$ for X_j are fixed at $\mu_j \equiv \beta_j$, which is characteristic to the *fixed II* model structure. In the *mixed* model structure this is seen for X_1, which therefore has the same effect on Y_g for every gene g. In this example all explanatory variables are continuous in both models. Any categorical explanatory variable (factor) X_j with K levels would lead to $K - 1$ fixed or random coefficients $\beta_{j_1g}, ..., \beta_{j_{K-1}g}$ or $b_{j_1g}, ..., b_{j_{K-1}g}$ for any gene g, respectively. Moreover, if the effect of that categorical X_j is random then it is possible to have a continuous $X_{j'}$ with a random intercept and slope with respect to X_j. In fact the *mixed* model structure (lower middle) is equivalent to another one (not shown), where "Gene" is a random factor X_{Gene} with random slope for the effects of X_2 and X_3.
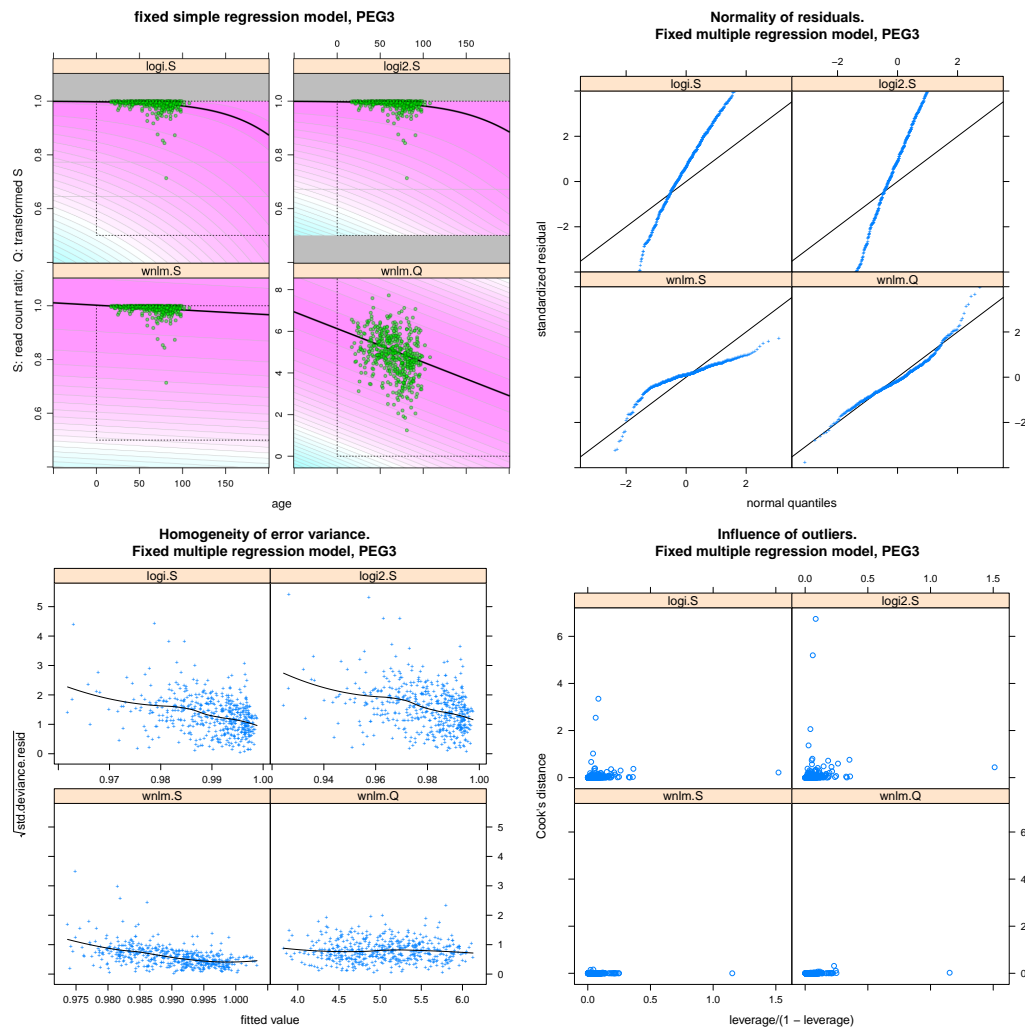
Figure S6: Fitting various fixed regression models, named logi.S, logi2.S, wnlm.S, wnlm.Q (Table S2), on the read count ratio data for the PEG3 gene. Results for models unlm.S, unlm.Q, unlm.R, wnlm.R are omitted for clarity and redundancy. In particular, unlm.Q gave as good fit as wnlm.Q. *Upper left:* Fitted curves (black lines) and sampling probabilities (magenta-white-cyan color gradient) of a version of the four models that is simple in the sense that Age is the only explanatory variable. Simple regression is used for this illustration only. For inference and all other plots in this figure multiple regression was performed, where Age is only one of several explanatory variables (Table S1). *Upper right (Normality of residuals):* analysis of the normality of the standardized residuals of fits suggests wnlm.Q is the best fitting model. *Lower left (Homogeneity of error variance):* Similar conclusion can be made by inspecting how the standardized deviance residuals depends on the fitted value. Goodness of fit is indicated by the lack of such dependence. Black curve: LOESS data smoother. *Lower right (Influence of outliers):* Influence of each individual on the fit quantified by Cook's distance (*y*-axis). This is plotted against a function of leverage, which quantifies a subcomponent of influence that is restricted to explanatory variables (i.e. individuals with extreme age, PMI,...). In ideal case all data points are expected to influence the fit to the same degree and thus have short Cook's distance.
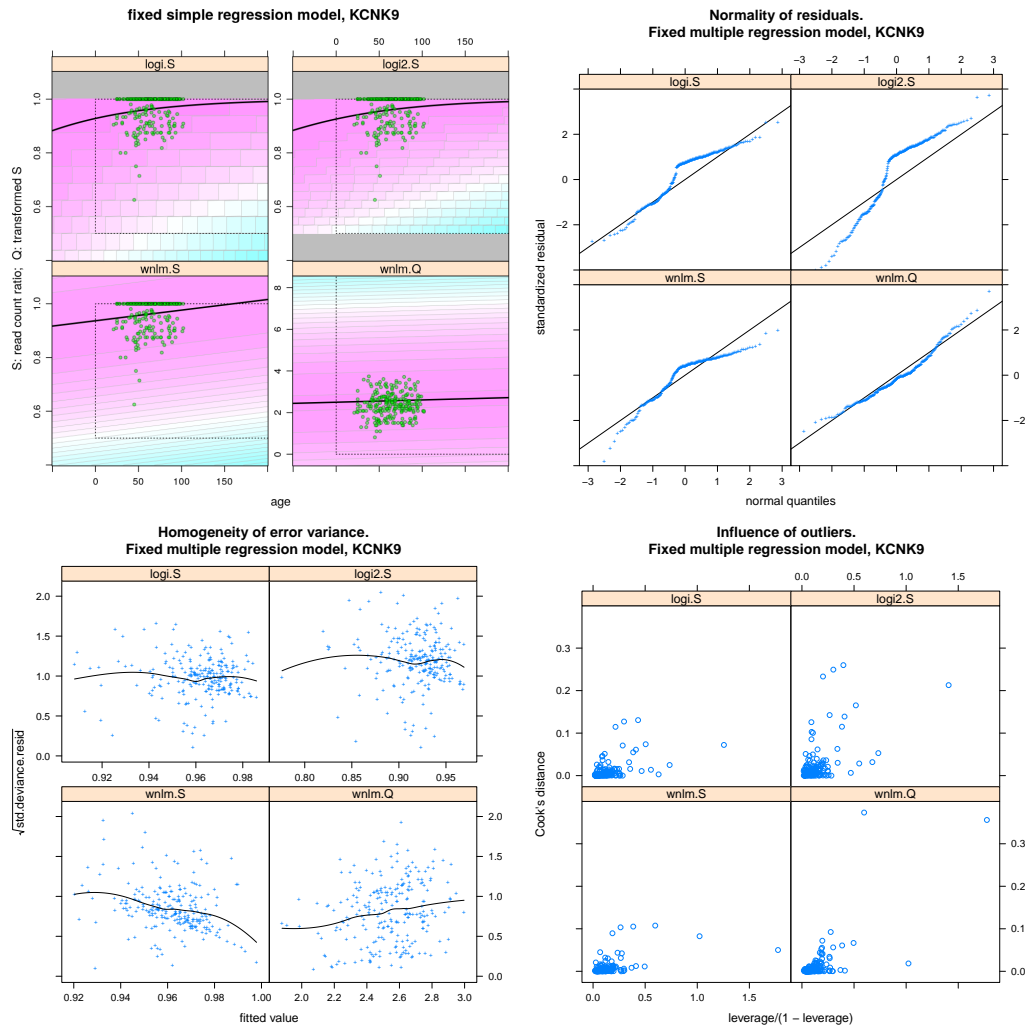
Figure S7: Fitting various fixed regression models on read count ratio data for the KCNK9 gene. See the legend of Fig. S6 for further details.
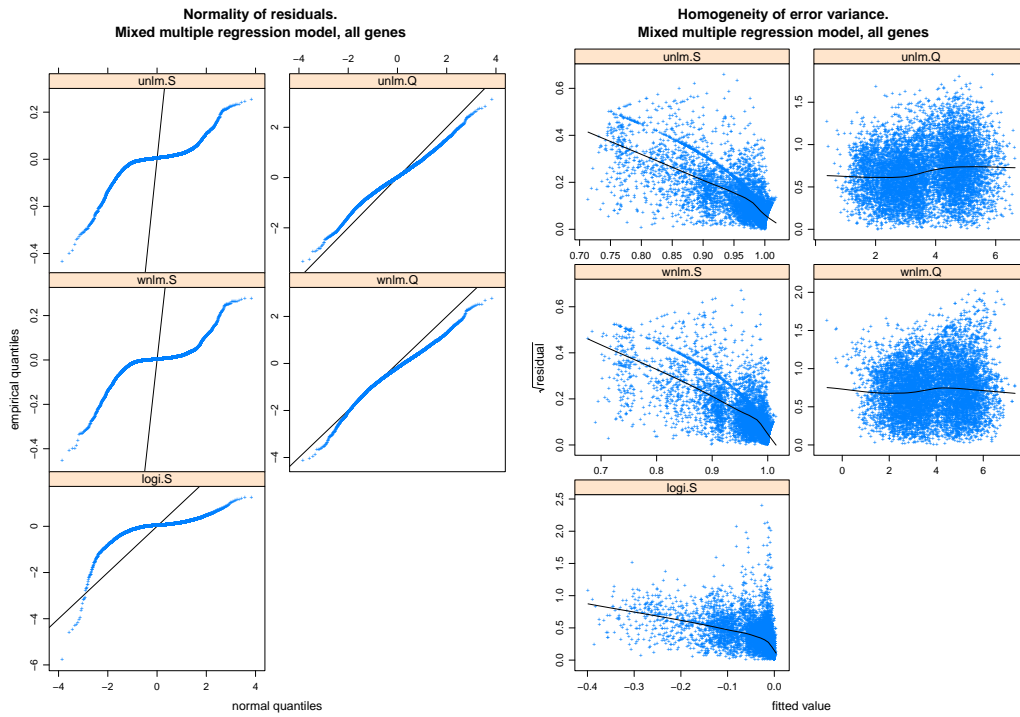
Figure S8: Fitting various mixed regression models, named logi.S, logi2.S, wnlm.S, wnlm.Q (Table S2), on the read count ratio data for all imprinted genes jointly. Results for models unlm.S, unlm.Q, unlm.R, wnlm.R are omitted for clarity. The plots suggest that unlm.Q and wnlm.Q fit the data the best. See the legend of Fig. S6 for further details. For its faster convergence (not shown) unlm.Q was selected as the favored model for statistical inference.
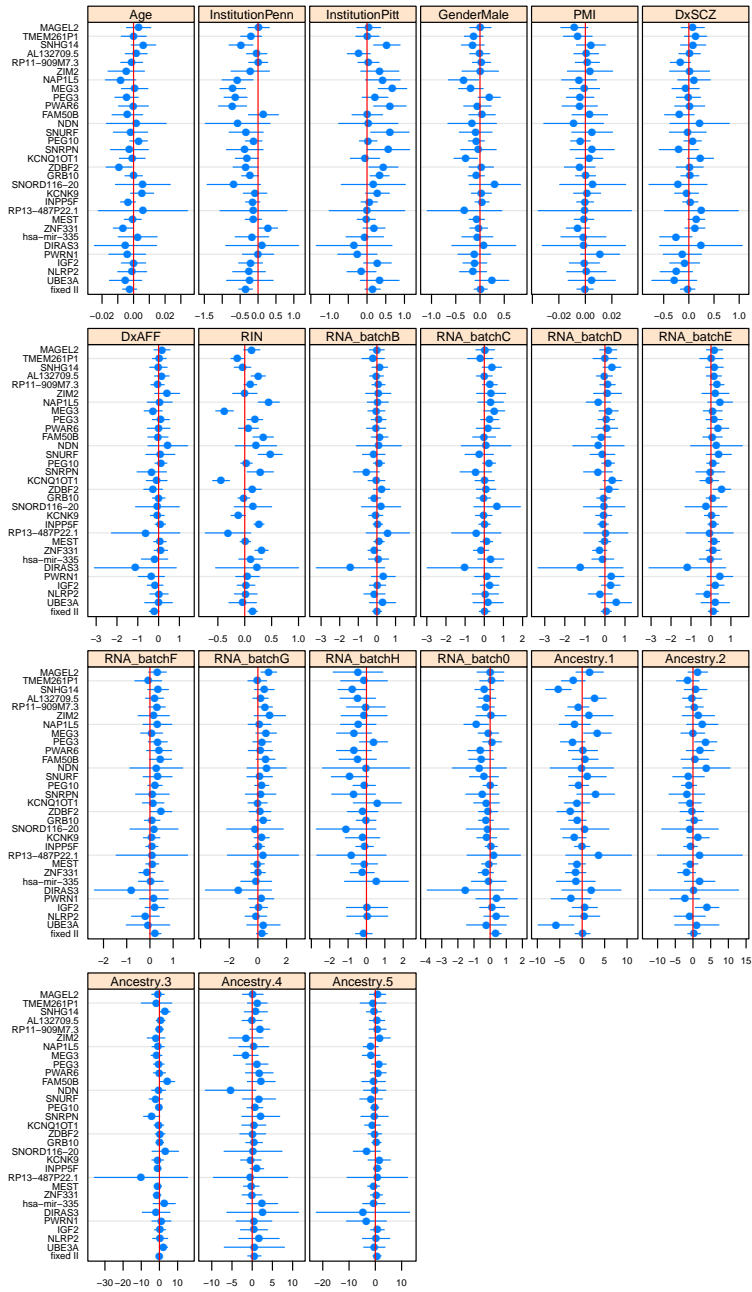
Figure S9: Estimated coefficients β_{jg} and 99% confidence intervals for gene g (y-axis) and fixed effect j (panel headers) under the *fixed I* model structure (Fig. S5). Below gene UBE3A the label fixed II indicates the gene-independent estimate under the *fixed II* model (Fig. S5). Positive and negative coefficient indicates direct positive and negative dependence of the given gene's read count ratio on age, respectively. Compare with Fig. 5 and S10.
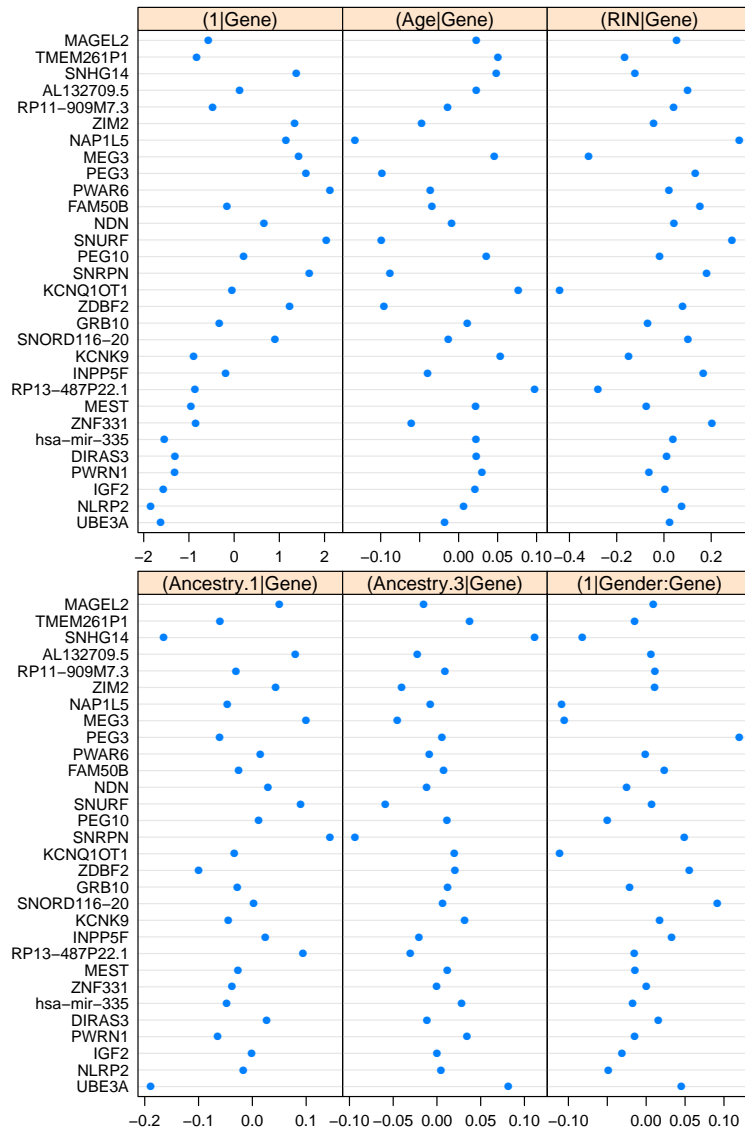
Figure S10: Predicted random coefficients b_{gj} for gene g (y-axis) and random effect j (panel headers) under the *mixed* model structure (Fig. S5). Positive and negative coefficient indicates direct positive and negative dependence of the given gene's read count ratio on age, respectively, while zero coefficient suggests independence of age. Compare with Fig. 5 and S9.

8.2 Supplementary tables with legends

explanatory variable	levels
Age	
Institution	[MSSM], Penn, Pitt
Gender	[Female], Male
PMI	
Dx	[Control], SCZ, AFF
RIN	
RNA_batch	[A], B, C, D, E, F, G, H, 0
Ancestry.1	
⋮	
Ancestry.5	

Table S1: *Left column:* explanatory variables of read count ratio. *Right column:* levels of each factor-valued (i.e. categorical) variable. Square brackets [...] surround the baseline level against which other levels are contrasted. *Abbreviations:* PMI: post-mortem interval; Dx: disease status; AFF: affective spectrum disorder; SCZ: schizophrenia; RIN: RNA integrity number; Ancestry.k: the k-th eigenvalue from the decomposition of genotypes indicating population structure.

model family	abbrev.	response var.
unweighted normal linear	unlm	S, Q, or R
weighted normal linear	wnlm	S, Q, or R
logistic	logi	S
logistic, $\frac{1}{2}\times$ down-scaled link fun.	logi2	S

Table S2: Fitted regression model families, in which the response variable is the read count ratio with or without some transformation: S—untransformed, Q—quasi-log-transformed, and R—rank-transformed read count ratio. Diagnostic plots (Fig. S8) and monitoring convergence suggested that the unlm.Q combination allows the best fit for several linear predictors tested.